Pure & Appl. Chem., Vol. 63, No. 6, pp. 873–878, 1991.
Printed in Great Britain.
© 1991 IUPAC
ADONIS 2069222091000965

Density functional theory as a practical tool for the study of elementary reaction steps in organometallic chemistry

Tom Ziegler

Department of Chemistry, University of Calgary, Calgary, Alberta T2N 1N4, Canada

Abstract - Approximate (A-DFT) Density Functional Theory is one out of a growing number of theoretical models by which one can study the dynamics and energetics of organometallic molecules. A-DFT calculations on a number of M-H, M-CH_3 and M-CO bond dissociation energies are shown to be in good agreement with experiment. and geometries optimized by the same method are seen to compare favourably with observations. It is finally shown how the method can trace the reaction profiles of elementary reaction steps in organometallic processes.

INTRODUCTION

A chemical process catalyzed homogeneously by transition metal complexes consists usually of several elementary steps connecting various intermediates. Some of the most frequently encountered steps are: Lewis base (or acid) ligand association/dissociation; reductive elimination /oxidative addition; insertion/extrusion; oxidative coupling/reductive decoupling as well as nucleophilic (or electrophilic) addition to unsaturated ligands. It is, however, not easy to determine the electronic structure and geometry of reaction intermediates (some of which must be rather short lived) or the precise mechanism for each elementary step in the catalytic cycle, including the transition state geometry. We shall here illustrate how theoretical calculations based on Density Functional Theory (Ref. *1a*) successfully can supplement experimental work on catalytic processes. Our investigation will be concerned with the structure and relative stability of intermediates involved in elementary processes along with the geometry of the possible associated transition states. Calculations will further be presented on metal-ligand bond energies. The dearth of reliable experimental data on bond dissociation energies is felt throughout the field of organometallic chemistry. Accurate theoretical studies should afford a much needed supplement to the sparse available experimental data on metal-ligand bond energies, necessary for a rational approach to the synthesis of new transition metal complexes.

Our calculations are based on Density Functional Theory (DFT) (Ref. *1a*) which over the past 10 years has emerged (Ref. 1b) as a tangible and versatile computational method in molecular science. The best known, and certainly the most simple DFT-based method is the Hartree-Fock-Slater (HFS) or Xα scheme. Recently, Density Functional investigations of molecular bond energies have gained novel impetus due to the introduction by Becke (Ref. *1c*) of a gradient correction to the Hartree-Fock-Slater local exchange expression (Ref .1a),

$$E_X^{LSD/NL} = E_X^{HFS} - \sum_\gamma \beta_B \int \frac{|\nabla_1 \rho_1^\gamma(\vec{r}_1)|^2}{[\rho_1^\gamma(\vec{r}_1)]^{7/3}} \left\{ 1 + \gamma_B \frac{|\nabla_1 \rho_1^\gamma(\vec{r}_1)|^2}{[\rho_1^\gamma(\vec{r}_1)]^{8/3}} \right\}^{-1} \delta\vec{r}_1 \qquad (1),$$

where ρ_1^γ is a spin density and β_B and γ_B are parameters. In conjunction with appropriate approximations for antiparallel spin correlations, the expression of Eq.(1) provides near-quantitative estimates (Ref. *1c*) of bond energies in main-group compounds and transition metal complexes . The method by Becke will be refered to as LSD/NL

COMPUTATIONAL DETAILS

In the present set of calculations we have used the functional proposed by Becke (Ref. *1*), which adopts a non-local correction to the HFS exchange, and treats correlation between electrons of different spins at the local density functional level. All calculations presented here were based on the LCAO-HFS program system due to Baerends *et al.* (Ref. *2*) or its relativistic extension due to Snijders *et al.*(Ref. *3*), with minor modifications to allow for Becke's non-local exchange correction as well as the correlation between electrons of different spins in the formulation by Stoll *et al.* (Ref. *4*) based on Vosko's parametrization (Ref. *5*) from homogeneous electron gas data. Bond energies were evaluated by the Generalized Transition State method (Ref. *6*), or its relativistic extensions (Ref. *7*).

A double ζ-STO basis (Ref. *8*) was employed for the *n*s and *n*p shells of the main group elements augmented with a single 3d STO function, except for Hydrogen where a 2p STO was used as polarization. The *n*s, *n*p, *n*d, (*n* + 1)s and (*n* + 1)p shells of the transition metals were represented by a triple ζ-STO basis (Ref. *8*). Electrons in shells of lower energy were considered as core and treated according to the procedure due to Baerends *et al.* (Ref. *2*). The total molecular electron density was fitted in each SCF-iteration by an auxiliary basis (Ref. *9*) of s, p, d, f and g STOs, centred on the different atoms, in order to represent the Coulomb and exchange potentials accurately.

BOND DISSOCIATION ENERGIES

The breaking or formation of metal-hydrogen and metal-alkyl bonds is an integral part of most elementary reaction steps in organometallic chemistry. As a consequence, considerable efforts have been directed toward the determination of M-H and M-alkyl bond strength (Ref. *10*) as a prerequisite for a full characterization of the reaction enthalpies of elementary steps in organometallic chemistry. A theoretical model of practical use in a quantitative study on reactivity must be able to represent such bond energies accurately and we compare in Table 1 theoretical (Refs. *14,11,12*) M-H and M-CH_3 bond dissociation energies with the available experimental data (Ref. *10*).

Table 1 Calculated and experimental values for the bond energies D(M-R) (R = H, CH_3) (kJ mol^{-1}).

M-H	LSD/NL[b]	Exp.[a]	M-CH_3	LSD/NL[b]	Exp.[a]
Cl_3Th-H	318.0	~335.	Cl_3Th-CH_3	333.9	~335.
Cl_3U-H	293.3	319.7	Cl_3U-CH_3	302.1	302.9
Cl_3Ti-H	250.7	—	Cl_3Ti-CH_3	267.5	—
Cl_3Zr-H	297.2	—	Cl_3Zr-CH_3	309.5	—
Cl_3Hf-H	313.5	—	Cl_3Hf-CH_3	326.6	—
H-$Mn(CO)_5$	225	213	CH_3-$Mn(CO)_5$	153	153
H-$Tc(CO)_5$	252	—	CH_3-$Tc(CO)_5$	178	—
H-$Re(CO)_5$	282	—	CH_3-$Re(CO)_5$	200	—
H-$Co(CO)_4$	230	238[c]	CH_3-$Co(CO)_4$	160	—
H-$Rh(CO)_4$	255	—	CH_3-$Rh(CO)_4$	190	—
H-$Ir(CO)_4$	286	—	CH_3-$Ir(CO)_4$	212	—

[a] Experimental bond energies from Ref. 10 .[b] Theoretical calculations from Ref 11-12.

The sparse experimental data indicate that the strengths of M-H and M-Alkyl bonds are comparable for early transition metals and f-block elements. By contrast, data for alkyl and hydride complexes of middle to late transition metals indicate that the M-H bond is stronger than the M-Alkyl bond by some 40-80 kJ mol^{-1}. We find in general a good agreement between the experimental bond energies and the theoretical values presented in Table 1. Also, the stability order D(M-L) > D(M-CH_3) for middle and late transition metal complexes is consistent with data on organometallic reactions in which M-L and M-CH_3 bonds are formed or broken. Thus, CO will readily insert into a M-CH_3 bond whereas the corresponding insertions into M-H bonds are virtually unknown (Ref. *13*), and methyl has likewise a larger migratory aptitude toward most other ligands than hydride. The H_2 molecule is known to add oxidatively and exothermically to several metal fragments where the corresponding oxidative additions of the H-Alkyl and Alkyl-Alkyl bonds are unknown and probably endothermic as a consequence of the weak M-R bond .

The reduced strength of the M-CH_3 bonds in middle and late transition metals can be readily explained (Ref. *11b*) in terms of destabilizing three- and four-electron two-orbital interactions which occur between the fully occupied methyl orbitals and the fully or singly occupied d-orbitals of matching symmetries present on the metal centres. By contrast, in early transition metal and actinide complexes, the metal orbitals of π-symmetry are vacant and are involved in stabilizing interactions with some of the occupied methyl orbitals. The comparable strengths of the M-H bonds in complexes of early as well as late transition metals within the same series is perhaps not too surprising, since H is a simple one-orbital ligand without additional occupied orbitals involved in four-electron two-orbital interactions . Finally, the increase in strength of both the M-H and M-CH_3 bonds down a triad, see Table 1, is primarily related to an increase in the metal-ligand overlap. Such an increase in overlap occurs as the metal d-orbitals become more diffuse down the triad.

The extensive use of coordinatively saturated mono-nuclear carbonyls as starting materials in organometallic chemistry, along with their volatility and high molecular symmetry, has prompted numerous experimental and theoretical studies on their structure and reactivity. Special attention has been given to the degree of σ-donation and π-back-donation in the synergic M-CO bond. However, in spite of many experimental investigations, there is still a lack of basic data on the thermal stability and kinetic lability of the M-CO bond in essential metal carbonyls such as $M(CO)_6$ (M = Cr, Mo, W), $M(CO)_5$ (M = Fe, Ru, Os) and $M(CO)_4$ (M = Ni, Pd, Pt), particularly with respect to the carbonyls of the second- and third-row metals. We compare in Table 2 theoretical (Ref. *14*) and experimental (Ref. *10*) values for the first CO dissociation enery

in a number of metal carbonyls. The first bond dissociation energy is an important kinetic parameter, since the dissociation process is assumed to be a key step in the large volume of kinetically useful substitution reactions. CO dissociation is also required to generate catalytically active and coordinatively unsaturated species. The calculated values given in Table 2 are seen to be in reasonable agreement with experiment.

Table 2 Comparison between calculated and experimental values for the first CO dissociation energy ΔH, values in kJ mol^{-1}. Calculated values do not include geometry relaxation of the fragments $M(CO)_{n-1}$.

$M(CO)_n$	LSD/NL[b]	Exp[a].	$M(CO)_n$	LSD/NL	Exp.
$Cr(CO)_6$	147	162[a]	$Fe(CO)_5$[b]	185[c]	176[d]
$Mo(CO)_6$	119	126[a]	$Ru(CO)_5$[b]	92	117[e]
$W(CO)_6$	142	166[a]	$Ni(CO)_4$	106	104[f]

[a] Experimental values from Ref. 10. [b] Calculated values from Ref. 14

A more extensive compilation of bond energies calculated by the LSD/NL method has been given elsewhere (Refs. 11-14).

MOLECULAR STRUCTURE

A theoretical method by which one should be able to study reaction mechanism must also be capable. of determining molecular structures. It has in recent years been possible to determine molecular structures by theoretical methods with increasing accuracy. Of particular importance in this development has been the implementation (Ref. 15), of automated procedures based on analytical expressions (Ref. 16) for the energy gradient. It is now routine to carry out geometry optimizations of organic molecules based on HF or correlated ab initio methods with an accuracy of ±.02 Å ,or better , for bond distances. The application of ab initio methods ,in particular on the HF-level, has been less successful in the area of transition metal chemistry (Ref. 17). This is illustrated by Table 3 where metal-carbon distances calculated by the HF-method with large basis sets are displayed for three representative organometallic molecules. The metal-carbon bond distances calculated by the HF-method are seen to be too long by up to .2 Å. The method gives in addition, in the case of $Fe(CO)_5$,a large difference of .2 Å between axial and equatorial bonds, which is not observed experimentally. The inability of the HF-method to supply reliable structural data for transition metal complexes can, as in the case of bond energies, be traced back to the near degeneracy error as discussed by Lüthi (Ref. 17) et al. The deficiency of the HF-method can be removed by configuration interaction methods. However, such methods are costly and less amenable to automated geometry optimization procedures based on analytical expressions

Table 3. A Comparison of Bond Distances (Å) from HF and HFS calculations with Experiment

	M-L	HF	HFS	Exp.
$Fe(CO)_5$	$Fe\text{-}C_{ax}$	2.047[a]	1.774[d]	1.807
	$Fe\text{-}C_{eq}$	1.874[a]	1.798[d]	1.827
$Fe(C_5H_5)_2$	Fe-C	1.88[b]	1.60[e]	1.65
$HCo(CO)_4$	$Co\text{-}C_{eq}$	2.02[c]	1.753[f]	1.764
	$Co\text{-}C_{ax}$	1.96[c]	1.779[f]	1.818

[a] Ref. 17a [b]Ref. 17b [c]Ref. 17c [d]Ref. 18a [e]Ref.18b [f]Ref. 18c

The geometrical parameters calculated (Ref. 18) by the simple DFT-based HFS-scheme are on the other hand seen to be in resonable agreement with experiment although the calculated bond-distances tend to be on the low side, Table 3. Automated procedures based on analytical expressions for the energy gradient have recently been implemented (Ref. *19*) within the DFT-framework. The optimized structures are in general (Ref. *19*) in excellent agreement with experiment. The energy gradient techniques have further been extended to the calculation of vibrational frequencies (Ref. *20*) and transition state structures (Ref. *21*).

ELEMENTARY REACTION STEPS

We have in the previous sections documented that DFT-based methods are able to provide information on bond energies and molecular geometries of reasonable accuracy. We shall in the ensuing sections illustrate how the same methods can be used to trace energy profiles for elementary reaction steps in organometallic.

Insertion of ethylene into the cobalt–hydrogen bond

Experimental findings suggest that the migration of a hydride to a coordinated olefin group is very facile. In fact, the hydride-olefin insertion reaction has, with a few exceptions, rarely been directly observed. As a consequence, metal complexes containing both hydride and olefin are scarce and it has only in a few cases been possible to study the insertion process by experimental techniques (Ref. 22). We have studied the insertion process (Ref. *23*), **1a** → **1b**, which is one of the key steps in the hydroformylation process.

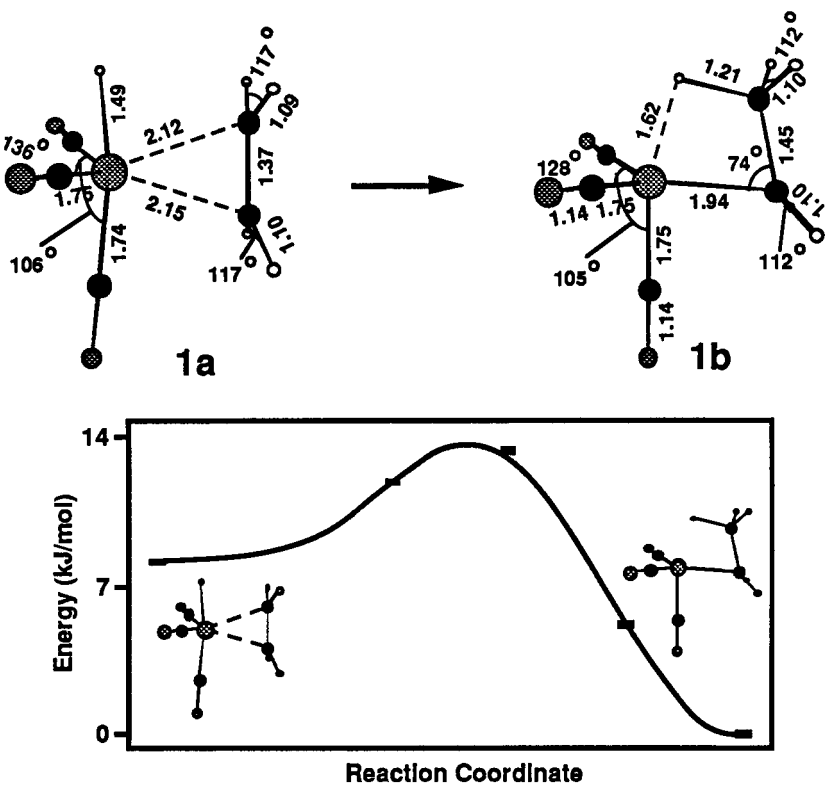

a) Reaction **1a** → **1b**. The energy zero point refers to structure **1b**

Figure 1. Energy profile of the hydride migration reaction **1a** → **1b** .

The energy profile for the reaction is given in Figure 1. We find the reaction to have a very small activation barrier ,$\Delta E^{\#}$,of only 6 kJ/mol and a modest reaction enthalpy of -8 kJ/mol. The product of the reaction is an ethyl-complex, **1b** , with a pronounced agostic interaction between the metal center and hydrogen. The ethyl-complex, **1b**, has a short metal-hydrogen distance of 1.62Å . This distance is only 0.12 Å longer than the Co-H bond distance in the parent complex **1a**. The bond length of the agostic hydrogen with the corresponding carbon atom of the ethyl ligand is, on the other hand, substantially elongated with R(H-C) = 1.21 Å in comparison to a normal ethyl C-H bond length of 1.11 Å. The C-C bond distance in the ethyl group is 1.45 Å, which is somewhat longer than the corresponding value in the parent structure **1a** (1.37 Å), but it is still substantially shorter than the C-C bond length of an undistorted ethyl group (1.53 Å). Also the bond angle Co-C_{et}-C_{et} is with 74° considerably smaller than the expected value of about 109° for a normal ethyl ligand. The optimized molecular parameters of structure **1b** clearly indicate that the π-bond character of the initial ethylene ligand has been retained to a large extent. This is also underlined by the small calculated energy difference of 8 kJ/mol between the parent structure **1a** and complex **1b**. The modest activation barrier found in this study stems from the fact that the hydrogen atom is close to cobalt throughout the migration reaction.

Migratory insertion of alkyl into the Co–CO bond

An other important elementary reaction step is the migratory insertion of alkyls into the metal-carbonyl bond. We have modeled (Ref. 18c) the migratory insertion process

$$RCo(CO)_4 \rightarrow RC(O)Co(CO)_3 \qquad (2),$$

which is an other important step in the hydroformylation cycle. The process in Eq. 2 could in principle proceed by an insertion of a CO into the Co-CH_3 bond of **2**, producing the coordinatively unsaturated complex, **3**, with the acyl group in an axial position. Alternatively, the methyl group might migrate to a cis-carbonyl thus affording the complex **4** with the acyl group in an equatorial position.

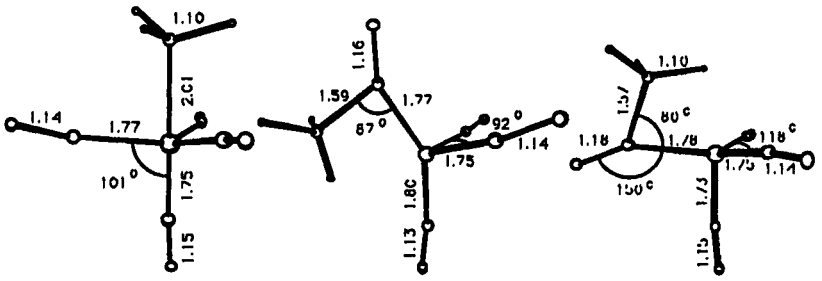

2 **3** **4**

We find, perhaps not surprisingly, that the energy profile for the CO insertion, **2** → **3**, into the Co-CH_3 bond, Figure 2a , has a prohibitively high activation barrier of 200 kJ/mol. The CO insertion can as a consequence not be a viable mechanism for the process in Eq. 2.

The migration of CH_3 to the cis-CO ligand,**2** → **4** , was calculated, Figure 2b, to have an endothermicity, ΔH, of 71 kJ/mol and a very modest activation barrier, $\Delta E^{\#}$, of only 9 kJ mol^{-1}. Thus the CH_3 migration ,**2** → **4** , seems to be favored as the mechanism for the process in Eq.2. The calculated reaction enthalpy and activation barrier for **2** → **4** compare well with an earlier study (Ref. 13) on the CH_3 to CO migration in $CH_3Mn(CO)_5$, where we found ΔH to be 75 kJ/mol and $\Delta E^{\#}$ 11 kJ/mol. Our findings are also in agreement with a recent kinetic study by Roe (Ref. 24), who found the rate constant of the methyl back migration of $CH_3C(O)Co(CO)_3$ to be considerably larger than the rate constant for the corresponding forward reaction. The structures in Figure 2b illustrate nicely how the methyl group can slide almost parallel along the cis C-Co bond onto the cis carbonyl carbon, while the remaining $Co(CO)_3$ framework stays almost unchanged. The 9 kJ/mol calculated for $\Delta E^{\#}$ in the present study is an upper bound to the actual value, and we can thus conclude that the methyl migration , **2** → **4** , should proceed with a rather modest activation barrier.

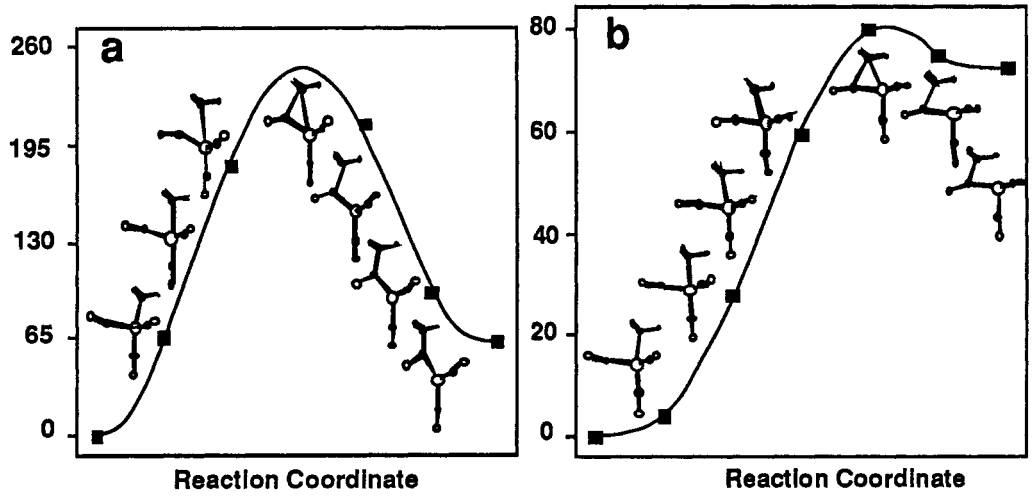

Figure 2. (a) Energy profile for the insertion of CO into the Co-CH_3 bond, **2** → **3**. (b) The energy profile for the migration of CH_3 to CO, **2** → **4**. The zero point refer to **2** in both plots

Other studies on elementary reaction steps

Other studies on elementary reaction steps include oxidative addition (Ref. 25) of H_2 to $Co(CO)_4$ as well as the oxidative addition (Ref. 26) of H_2 and CH_4 to CpML (L=CO,PH_3;M=Rh,Ir). Polymerization of organosilanes (Ref. 27) and halogen abstraction by metal carbonyl anions (Ref. 28). Investigations have in addition been carried out on the insertion of aldehydes into the Co-H bond (Ref. 29) , the metathetical exchange reactions between Cp_2LuR (R=H,CH_3) and H_2 or CH_4 (Ref.30) as well as the insertion (Ref. 31) of olefins into the Lu-R bond (R=H,CH_3) . The optimization of transition states structures by DFT has been discussed in Ref. 32.

Acknowledgement This investigation was supported by the Natural Sciences and Engineering Research Council of Canada (NSERC).

REFERENCES

1. (a) Parr,R.G.;Yang,W. Density Functional Theory of Atoms and Molecules; Oxford University Press.1989
   (b) Ziegler,T. Chem.Rew. 1991,in press
   (c) Becke, A.D. *J. Chem. Phys.* **1986**, *84*, 4524.
2. Baerends, E.J.; Ellis, D.E.; Ros, P. *Chem. Phys.* **1973**, 2, 71.
3. Snijders, J.G.; Baerends, E.J.; D.E.; Ros, P. *Molec. Phys.* **1979**, *38*, 1909.
4. Stoll, H.; Golka, E.; Preuss, H. *Theor. Chim. Acta* **1980**, *55*, 29.
5. Vosko, S.H.; Wilk, L.; Nusair, M. *Can. J. Phys.* **1980**, *58*, 1200.
6. Ziegler, T.; Rauk, A. *Theor. Chim. Acta* **1977**, *46*, 1.
7. Ziegler, T.; Snijders, J.G.; Baerends, E.J. *J. Chem. Phys.* **1981**, *74*, 1271.
8. (a) Snijders, J.G.; Baerends, E.J.; Versnoijs, P. *At. Nucl. Data Tables* **1982**, *26*, 483.
   (b) Versnoijs, P.; Snijders, J.G.; Baerends, E.J. *Slater Type Basis Functions for theWhole Periodic System.* Internal Report; Free University: Amsterdam, 1981.
9. Krijn, J.; Baerends, E.J. *Fit Functions in the HFS-method.* Internal Report (in Dutch); Free University: Amsterdam, 1981.
10. (a) Halpern, J. *Acc. Chem. Res.* **1982**, *15*, 238.
    (b) Martinho Simoes,J.A.; Beauchamp,J.L. Chem.Rew. **1990**,
11. (a) Ziegler, T.; Tschinke, V.; Baerends, E.J.; Snijders, J.G. *J. Phys. Chem.* in press.
    (b) Ziegler, T.; Tschinke, V.; Becke, A. *J. Am. Chem. Soc.* **1987**, *109*, 1351.
12. Ziegler, T.; Wendan, C.; Baerends, E.J.; Ravenek, W. *Inorg. Chem.* **1988**, *27*, 3458.
13. Ziegler, T.; Versluis, L.; Tschinke, V. *J. Am. Chem. Soc.* **1986**, *108*, 612.
14 Ziegler, T.; Tschinke, V.; Ursenbach, C. *J. Am. Chem. Soc.* **1987**, *109*, 4825.
15. Hehre,W.J.;Radom,L.;Schleyer,P.W.R.;Pople,J.A. in Ab initio Molecular Theory ,Wiley,New York,**1986.**
16 Pople,J.A.;Krishnan,R.;Schlegel,H.B.;Binkley,J.S. Int.J.Quantum Chem. **1979**,S13,225
17. (a) Lüthi,H.P.;Siegbahn,P.E.M.;Almlöf,J. J.Phys.Chem. **1985**,89,2156
    (b) Lüthi,H.P.;Ammeter,J.A.;Almlöf,J.;Faegri,K. *J.Chem.Phys.* **1982**,77,2002
    (c) Antolovic,D.;Davidson,E.R. *J.Chem.Phys.* **1988**,88,4967
18. (a) Rösch,N.;Jorg,H;Dunlap,B.I. NATO ASI **1985**,176,179
    b) Dunlap,B.I. J.Phys.Chem. **1986**,90,5524
    (c) Versluis,L.; Ziegler,T. *J.Am.Chem.Soc.* **1989**,111,2018
19. (a) Fournier,R.;Andzelm,J.;Salahub,D.R. *J.Chem.Phys.* **1989**,90,6371
    (b) Versluis,L.;Ziegler,T. *J.Chem.Phys.* **1988**, 88,322
20. (a) Fan,L.;Versluis,L.;Ziegler,T.;Baerends,E.J.;Ravenek,W. Int. J. Quantum Chem. **1988**,S22,173
    (b) St-Amant,A.;Fournier,R.;Salahub,D.R. Int. J.Quantum Chem. **1989**,S23,
21. Fan,L.;Ziegler,T. J.Chem.Phys. **1990**,92,3645
22. Werner,H.;Feser,R. Angew.Chem.Int.Ed.Engl. **1979**,18,57
23. Versluis,L.;Ziegler,T. Inorg.Chem. **1990**, in press
24. Roe,D.C. Organometallics **1987**, 6, 942
25. Versluis,L.;Ziegler,T.., Organometallics, **1990**, in press.
26. Ziegler,T.;Tschinke,V.;Fan,L.;Becke,A.D. J.Am.Chem.Soc. **1989**,111,9177
27. Harrod,J.F.;Tschinke,V. Organometallics , 1990,9,897.
28. Masters,A.P.;Soerensen,T.S.;Ziegler,T.. , Organometallics, **1989**,8,1088.
29 Versluis,L.;Ziegler,T. ,J.Am.Chem.Soc.,**1990**,112,in press.
30. Folga.E.;Ziegler,T. Organometallics, submitted.
31. Tschinke,V.;Folga,E.;Ziegler,T. ,Organometallics,submitted
32. Fan,L.;Ziegler,T., J.Chem.Phys., **1990**,92,897